Functional changes in the language network in response to increased amyloid β deposition in cognitively intact older adults

Katarzyna Adamczuk[1,2], An-Sofie De Weer[1], Natalie Nelissen[1,3], Patrick Dupont[1,2], Stefan Sunaert[2,4], Karolien Bettens[5,6], Kristel Sleegers[5,6], Christine Van Broeckhoven[5,6], Koen Van Laere[2,7], Rik Vandenberghe[1,2,8]

[1]Laboratory for Cognitive Neurology, KU Leuven, Belgium; [2]Alzheimer Research Centre KU Leuven, Leuven Institute of Neurodegenerative Disorders, KU Leuven, Belgium; [3]Department of Experimental Psychology, Oxford University, UK; [4]Radiology Department, KU Leuven and UZ Leuven, Belgium; [5]Neurodegenerative Brain Diseases group, VIB Department of Molecular Genetics, Antwerp, Belgium; [6]Laboratory of Neurogenetics, Institute Born-Bunge, University of Antwerp, Belgium; [7]Nuclear Medicine and Molecular Imaging Department, KU Leuven and UZ Leuven, Belgium; [8]Neurology Department, UZ Leuven, Belgium

Corresponding author: Rik Vandenberghe, MD, PhD, Neurology Department, University Hospitals Leuven, Herestraat 49, 3000 Leuven, Belgium. E-mail: rik.vandenberghe@uz.kuleuven.ac.be.

Keywords (up to 5): fMRI, amyloid PET, semantic, ^{18}F-flutemetamol, Alzheimer

Cerebral Cortex 2014; DOI: 10.1093/cercor/bhu286

Abstract

Word finding symptoms are frequent early in the course of Alzheimer's disease and relate principally to functional changes in left posterior temporal cortex. In cognitively intact older adults, we examined whether amyloid load affects the network for language and associative-semantic processing. Fifty-six community-recruited subjects (52-74 years), stratified for Apolipoprotein E and Brain Derived Neurotrophic Factor genotype, received a neurolinguistic assessment, ^{18}F-flutemetamol PET, and a functional MRI of the associative-semantic system. The primary measure of amyloid load was the cerebral-to-cerebellar grey matter standardized uptake value ratio in a composite cortical volume of interest ($SUVR_{comp}$). The primary outcome analysis consisted of a whole-brain voxelwise linear regression between $SUVR_{comp}$ and fMRI response during associative-semantic versus visuoperceptual processing. Higher activity in one region, the posterior left middle temporal gyrus, correlated positively with increased amyloid load. The correlation remained significant when only the word conditions were contrasted but not for pictures. According to a stepwise linear regression analysis, offline naming reaction times correlated positively with $SUVR_{comp}$. A binary classification into amyloid-positive and amyloid-negative cases confirmed our findings. The left posterior temporal activity increase may reflect higher demands for semantic control in the presence of a higher amyloid burden.

1 Introduction

Modern techniques such as amyloid positron emission tomography (PET) allow one to detect hallmark lesions related to Alzheimer's disease (AD) directly in vivo (Clark et al. 2011; Herholz and Ebmeier 2011; Clark et al. 2012; Vandenberghe et al. 2013c, 2013d). Depending on mainly age and Apolipoprotein E (APOE) genotype, 10-30% of cognitively intact older adults have a positive amyloid scan, which can be indistinguishable from what is seen in clinically probable AD (for review see Chételat et al. 2013). Longitudinally, increased Aβ load is associated with greater risk of cognitive decline (Morris et al. 2009; Resnick et al. 2010; Villemagne et al. 2011; Doraiswamy et al. 2012) and grey matter volume loss (Chételat et al. 2012). Amyloid PET has become one of the principal ways to define the 'preclinical' stage of AD, a term that refers to the AD-related pathogenetic processes that happen before clinical symptoms become apparent (Sperling et al. 2011). In this study we used ^{18}F-flutemetamol (Vandenberghe et al. 2010) as our ligand. Previous studies have revealed a high correlation between the cortical retention levels obtained with this ligand and those obtained with ^{11}C-Pittsburgh Compound B (Vandenberghe et al. 2010; Hatashita et al. 2014) as well as with neuritic plaque density based on Bielschowsky silver staining (Thurfjell et al. 2014).

Word finding difficulties are frequent in clinically probable AD, even at a pre-dementia stage (Bayles and Tomoeda 1983; Huff et al. 1986; Chertkow and Bub 1990; Vandenbulcke et al. 2007; Apostolova et al. 2008; Clark et al. 2009; Sugarman et al. 2012). The first language area to become dysfunctional in early-stage AD and amnestic mild cognitive impairment (MCI) is the left posterior superior temporal sulcus (STS) (Nelissen et al. 2007; Vandenbulcke et al. 2007). Functional magnetic resonance imaging (fMRI) activity is lower in this region during associative-semantic compared with visuoperceptual processing in MCI patients (Vandenbulcke et al. 2007) and in clinically probable AD (Nelissen et al. 2007) compared to controls. In these populations, fMRI activity levels positively correlate with Boston Naming test scores (Nelissen et al. 2007) and with word identification speed (Vandenbulcke et al. 2007). Furthermore, in AD patients in whom naming is preserved, fMRI activity in the homotopical right-sided STS is increased compared to controls (Nelissen et al. 2007). Accordingly, we hypothesized that posterior temporal cortex may show adaptive changes in the presence of increased amyloid burden also in cognitively intact individuals. The study of functional changes related to amyloid burden in cognitively intact subjects is important because it could explain why some brains appear to be more resilient against Aβ related injury than others. This factor may determine which individuals show clinical manifestations of underlying Alzheimer pathology and who remain cognitively intact despite the presence of Alzheimer pathology in the brain (Crystal et al. 1988; Katzman et al. 1988; Troncoso et al. 1996; Davis et al. 1999; Price and Morris 1999; Driscoll et al. 2006; Aizenstein et al. 2008). Even during the initial stages of neurodegenerative disease, the brain retains a potential for plasticity (Hyman et al. 1987; Nathan et al. 1994; Becker et al. 1996; Arendt et al. 1997; Mesulam 1999; Saykin et al. 1999; Grady et al. 2001; Grossman et al. 2003b).

One of the genes that have been implicated in functional plasticity (Gorski et al. 2003; Webster et al. 2006) is Brain Derived Neurotrophic Factor (BDNF), both in humans (Erickson et al. 2011) and in animal models (Okuno et al. 1999; Li et al. 2008; Osada et al. 2008). The presence of one or two *met* alleles on codon 66 is often considered to reduce the capacity for functional reorganisation. As our second hypothesis, we examined whether adaptive changes occurring in the language network in response to amyloid load differ

between BDNF *met* carriers and non-carriers and how this interacts with APOE ε4 genotype (Adamczuk et al. 2013).

2 Materials and methods

The protocol was approved by the Ethics Committee University Hospitals Leuven (EudraCT: 2009-014475-45) and written informed consent was obtained from all subjects in accordance with the latest version of the Declaration of Helsinki.

2.1 Participants

Subjects were recruited from the community via advertisement in local newspapers and via a website for seniors, asking for healthy volunteers between 50 and 75 years of age for participation in a scientific study at the University Hospital Leuven, Belgium, involving brain imaging. The relationship between genotype (APOE versus BDNF) and amyloid levels in the present cohort has been described by Adamczuk et al. (2013).

At screening, subjects underwent blood sampling for genotyping, Mini Mental State Examination (MMSE), Clinical Dementia Rating score (CDR), and a structured interview about medical history. Inclusion was stratified per age bin (50-59, 60-64, 65-69, 70-75) for two genetic factors: BDNF (*met* allele present or absent) and APOE (ε4 allele present or absent). The cells of this 2 x 2 factorial design were prospectively matched for number of cases, gender, age, education and handedness (Edinburgh Handedness Inventory) (Adamczuk et al. 2013). BDNF and APOE variants were genotyped by sequencing at the Genetic Service Facility (GSF, www.vibgeneticservicefacility.be) of the VIB Department of Molecular Genetics. The study exclusion criteria were an MMSE score below 27, a CDR score above 0, neurological or psychiatric history, brain lesions on structural MRI, left-handedness, non-native Dutch speaker, and below-normal test scores on conventional neuropsychological assessment (< 1.9 SD on published norms adapted for age, gender, and education) (Table 1). The conventional neuropsychological test protocol consisted of the Rey Auditory Verbal Learning Test, Boston Naming Test, Letter Verbal Fluency and Animal Verbal Fluency, Raven's Standard Progressive Matrices and the Trail Making Test (Table 1).

Fifty-six healthy, right-handed adults between 50 and 75 years of age (mean age = 65, SD = 5.5, range 52-74) who fulfilled all criteria were included in the study.

2.2 Experimental language tests

Given our a priori hypothesis of early involvement of left posterior STS and given its possible role in lexical-semantic retrieval (Vandenbulcke et al. 2007), the experimental language tests conducted outside the fMRI scanner consisted of confrontation naming, lexical decision and speeded word identification (Table 2). Each of these tests was presented by Presentation 14.8 (NeuroBehavioural Systems, Albany, CA, USA) and was displayed on a 19-inch cathode ray tube monitor (resolution 1024 x 768 pixels, refresh rate 75 Hz) 60 cm from subjects' eyes.

Table 1

Demographic data and neuropsychological test scores

	Genetic groups				*P*
BDNF	*met+*	*met-*	*met+*	*met-*	
APOE	ε4+	ε4+	ε4-	ε4-	
Gender (M/F)	7/7	7/4	7/7	10/7	0.9
Age (years)	64.7 (5.9)	66.5 (4.7)	64.5 (6.0)	64.9 (5.5)	0.83
Education (years)	13.1 (2.7)	12.7 (1.8)	13.8 (2.2)	14.4 (3.6)	0.47
Handedness	94.3 (15.5)	100.0 (0.0)	96.2 (8.2)	100.0 (0.0)	0.24
MMSE (/30)	28.9 (0.9)	28.7 (1.1)	29.3 (0.6)	28.9 (0.9)	0.47
AVLT TL (/75)	48.7 (8.0)	47.5 (8.4)	51.2 (12.4)	50.0 (8.4)	0.79
AVLT DR (/15)	11.6 (2.2)	9.0 (3.3)	11.4 (2.7)	10.8 (2.1)	0.07
BNT (/60)	53.6 (4.6)	50.9 (7.4)	53.4 (3.9)	54.0 (3.3)	0.39
AVF (# words)	18.6 (4.7)	19.7 (5.2)	21.9 (5.8)	21.3 (4.3)	0.30
LVF (# words)	32.4 (12.1)	29.8 (7.9)	34.1 (10.3)	37.1 (10.0)	0.33
RPM (/60)	39.1 (9.2)	39.8 (8.7)	45.7 (6.6)	46.5 (7.5)	0.03
TMT B/A	2.9 (1.1)	2.4 (0.6)	2.5 (0.9)	2.5 (1.1)	0.50

Note: Values represent means and standard deviations. Gender is expressed in number of individuals. M = male; F = female; MMSE = Mini Mental State Examination; AVLT = Rey Auditory Verbal Learning Test; TL = total learning; DR = delayed recall; BNT = Boston Naming Test; AVF = Animal Verbal Fluency Test; LVF = Letter Verbal Fluency Test; RPM = Raven's Progressive Matrices; TMT = Trail Making Test B divided by A. Last column represents *P*-values for one-way between groups ANOVA. Bonferroni corrected threshold for significance $P < 0.006$ corresponding to $P_{corrected} < 0.05$.

2.2.1 Confrontation naming task

In a computerized version of the picture naming task from Laiacona and Capitani (Laiacona and Capitani 2001), 60 white line drawings of concrete entities were presented on a black background (picture size 9.68 deg x 7.74 deg; Snodgrass and Vanderwart 1980). The 60 items comprised 3 living (10 animals, 10 fruits and 10 vegetables) and 3 non-living (10 tools, 10 pieces of furniture, 10 vehicles) categories. Item order was randomized for each individual. A trial started with the appearance of a fixation point displayed for 2 s before stimulus onset. A warning sound (177 ms duration) was presented 500 ms before stimulus onset. The stimulus was on the screen until the subject provided a response, for a maximum duration of one minute.

Reaction times (RT) were measured for the correct responses from the onset of the stimulus to the onset of the naming response. Voice recordings were manually analysed in the

WavePad Sound Editor version 4.57 (http://www.nch.com.au/wavepad). Accuracy was measured as percentage correct responses. Responses were considered correct if they were the picture's dominant name, a synonym, the name of a subordinate to the entity designated by the dominant name, or else if it occurred in at least 3 out of 30 other healthy controls viewing the picture for 2 s. Spontaneous, immediate auto-corrections were allowed.

Table 2

Experimental test scores

		Genetic groups				*P*		
	BDNF	*met+*	*met-*	*met+*	*met-*			
	APOE	ε4+	ε4+	ε4-	ε4-	*BDNF*	*APOE*	*Int*
Conf naming	RT (ms)	1595 (288)	1507 (237)	1471 (333)	1450 (317)	0.27	0.50	0.68
	Accu (%)	93.0 (3.3)	91.2 (8.1)	92.4 (5.3)	90.7 (5.0)	0.70	0.24	0.96
Lexical decision	RT (ms)	1033 (146)	1118 (238)	1138 (211)	1154 (352)	0.29	0.44	0.60
	Accu (A')	0.99 (0.01)	0.99 (0.01)	0.99 (0.01)	0.98 (0.02)	0.95	0.38	0.45
Speeded id W	*a* (ms)	25.2 (17.5)	21.2 (9.7)	21.6 (12.2)	19.9 (9.1)	0.48	0.42	0.75
	b (ms)	17.4 (8.3)	25.5 (13.5)	22.7 (10.1)	19.2 (10.7)	0.85	0.42	0.05
	c (%)	99.1 (1.3)	98.2 (1.8)	99.6 (0.6)	99.0 (1.7)	0.09	0.05	0.77

Note: Values represent means and standard deviations. Conf naming = confrontation naming task; Speeded id W = speeded identification task for words; RT = reaction times; Accu = accuracy. Last three columns represent significant values for the main effect of BDNF, APOE, and interaction between them. Bonferroni corrected threshold for significance $P<0.007$ corresponding to $P_{corrected}<0.05$.

2.2.2 Lexical decision task

In a computerized version of the visual lexical decision test from the Dutch version of the Psycholinguistic Assessment of Language Processing in Aphasia (PALPA 24, Bastiaanse et al. 1995), words and non-words were presented as white letters (letter height: 1 deg) on a black background. Stimuli consisted of 40 words with high imageability (20 high and 20 low frequency words), 40 words with low imageability (20 high and 20 low frequency words) and 80 non-words, randomly divided into 4 blocks (literal transcription of PALPA 24 paper version). Each stimulus was preceded by a fixation point for 1 s. Subjects were instructed to use their dominant hand and respond by key press whether the stimulus was a word or non-word. The stimulus was on the screen until the subject responded, for a maximum duration of stimulus presentation of 30 s.

RTs were measured for correct responses from the onset of the stimulus to the time of the button press. A' was used as our accuracy measure (Pallier 2002).

2.2.3 Speeded word and picture identification

The purpose of the speeded word and picture identification task was to analyse written word and picture identification under varying time constraints (Vandenbulcke et al. 2007). We

derived a time-accuracy curve for stimulus presentation durations varying between 30, 60, 90, 150, 200, 500, 800 or 2000 ms. Subjects were instructed to read the word or name the picture. A trial consisted of a warning sound, a forward mask (200 ms duration, 9.68 deg x 7.74 deg), followed by either a word (letter height 1 deg) or a picture (9.68 deg x 7.74 deg; Snodgrass and Vanderwart 1980), which was immediately followed by a backward mask (200 ms duration, 9.68 deg x 7.74 deg), and a fixation point for 3 s. For each individual subject, the onset (*a*), steepness of the curve (*b*), and asymptote (*c*) of the time-accuracy function for words and pictures were calculated by means of the equation: $accuracy = c*(1-e^{(a-\Delta t)/b})$ for $\Delta t \geq a$ (Verhaeghen et al. 1998; Vandenbulcke et al. 2007). Goodness of fit was estimated as the sum of squared differences between the measured and calculated values (sum of the squared errors).

2.3 Functional MRI

2.3.1 Stimuli and tasks

Stimuli were projected onto a screen (resolution of 1024 x 768 pixels, refresh rate 60 hz) using Presentation 14.8 (NeuroBehavioural Systems, Albany, CA, USA). The fMRI paradigm has been described in detail before (Vandenberghe et al. 1996; Vandenbulcke et al. 2005, 2006; Nelissen et al. 2007; Vandenbulcke et al. 2007; Nelissen et al. 2011; Vandenberghe et al. 2013a). In summary, the experimental design was factorial (Vandenberghe et al. 1996). The first factor, task, had two levels: associative-semantic (Fig. 1 blue and purple) versus visuoperceptual judgement (Fig. 1 cyan and yellow). The second factor, input modality, also had two levels: printed words (Fig. 1 blue and cyan) versus pictures (Fig. 1 purple and yellow). The associative-semantic condition was derived from the Pyramids and Palm Trees test (Howard and Patterson 1992), a classical neuropsychological test of associative-semantic processing for words and pictures. During a trial, a triplet of stimuli was presented

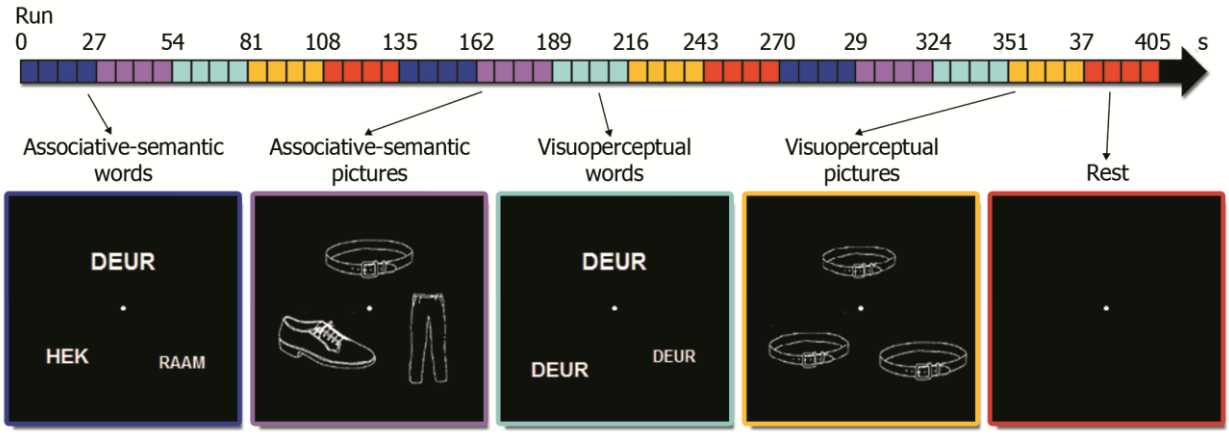

Figure 1: Stimuli and tasks in fMRI experiment. Associative-semantic task with words (*blue*) and with pictures (*purple*). Visuoperceptual task with words (*cyan*) or pictures (*yellow*). Resting baseline with fixation point (*red*). Subjects were asked to press a left- or right-hand key depending on which of the two lower stimuli matched the upper stimulus more closely in meaning (*blue, purple*) or in size on the screen (*cyan, yellow*). A given concept triplet was presented in either the word or the picture format and this was counterbalanced across subjects. Arrow in the top of the figure shows a timeline of one fMRI run, with each condition indicated in its respective colour. The order of conditions was randomized for each run and subject. Translation: deur = door, hek = fence, raam = window.

for 5250 ms, one stimulus on top (the sample stimulus) and one in each lower quadrant (the test stimuli) at 4.6 deg eccentricity (mean picture size was 3.7 deg and mean letter size 1.2 deg), followed by a 1500 ms interstimulus interval. Subjects were asked to press a left- or right-hand key depending on which of the two test stimuli matched the sample stimulus more closely in meaning. A given triplet was presented in either the picture or the word format and this was counterbalanced across subjects. In the visuoperceptual control condition, a picture or word stimulus was presented in three different sizes (mean picture size was 3.7 deg and mean letter size 1.2 deg). Subjects had to press a left- or right-hand key depending on which of the two test stimuli matched the sample stimulus more closely in size on the screen. An epoch, i.e. a block of trials belonging to the same condition, consisted of four trials (total duration 27 s). The fifth condition consisted of a resting baseline condition during which a fixation point was presented in the centre of the screen (Fig. 1 red). During each fMRI run (5 runs in total), a series of the 5 epoch types, was replicated 3 times (Fig. 1 timeline). The order of conditions was pseudorandom and different across runs of the same subject.

Prior to the fMRI session, visual acuity was tested in each participant. Subjects were asked to read aloud a text written in font 12 at 40 cm distance from their eyes. In case a correction to normal vision was necessary, subjects received MR compatible glasses with lenses matched to the subjects' sight defect. Following this, subjects performed an offline practice session of fMRI task. In this session we determined which size difference (9%, 6%, 3%, or 1%) for the visuoperceptual conditions was needed for each individual subject to obtain comparable accuracies as for the associative-semantic conditions.

2.3.2 Image acquisition

Twenty-eight subjects were scanned on a 3T Philips Intera system equipped with an 8-channel receive-only head coil (Philips SENSitivity Encoding head coil). Twenty-eight subjects could not undergo the fMRI in the Intera system because their body in the scanner lumen obstructed the beam from the projector to the screen. These subjects were scanned on a 3T Philips Achieva system equipped with a 32-channel receive-only head coil (Philips SENSitivity Encoding head coil) which used a screen placed behind the individual's head for the projection. There were no statistically significant differences of sex ($P = 0.79$) (*chi* square test), genetic groups ($P = 0.17$), age ($P = 0.49$), or MMSE ($P = 0.92$) (Kolmogorov-Smirnov comparison of two datasets) between subjects scanned on the Intera versus the Achieva system. Scanner type was included as a covariate of no interest for all analyses.

Sequence parameters were the same for both scanners. A high-resolution T1-weighted structural scan was obtained using a 3D turbo field echo sequence (coronal inversion recovery prepared 3D gradient-echo images, inversion time 900 ms, TR = 9.6 ms, TE = 4.6 ms, flip angle 8°, field of view = 250 x 250 mm, 182 slices; voxel size 0.98 x 0.98 x 1.2 mm^3). Functional MRIs were acquired using T2* echo-planar images (50 transverse slices, voxel size 2.5 x 2.5 x 2.5 mm^3; TR = 3000 ms, TE = 30ms, flip angle 90°, field of view 200 x 200 mm).

2.3.3 Image analysis

All analyses were performed using Statistical Parametric Mapping 8 (SPM8, http://www.fil.ion.ucl.ac.uk/spm). Functional MR scans of each subject were realigned to correct for potential head motion. The structural MR image was coregistered to the average of the realigned fMRI images. The structural MR image was then normalized to the SPM8 T1

template in Montreal Neurological Institute (MNI) space. The same normalization matrix was applied to the coregistered fMRI scans. The normalized fMRI images (voxel size 3 x 3 x 3 mm^3) were smoothed using a 6 x 6 x 6 mm^3 Gaussian kernel. A high- pass filter with a Full Width at Half Maximum of 270 s and a low-pass filter consisting of a canonical hemodynamic response function (HRF) were applied. The epoch-related response was modeled by a canonical HRF convolved with a boxcar.

2.4 Flutemetamol PET

2.4.1 Image acquisition

As described before (Koole et al. 2009; Nelissen et al. 2009; Vandenberghe et al. 2010, 2013b), images were acquired on a 16-slice Siemens Biograph PET/CT scanner (Siemens, Erlangen, Germany). The PET tracer was injected intravenously as a bolus (mean activity 151.2 MBq, SD 8.3, range 137.9 - 192.5 MBq) in an antecubital vein. Image acquisition started 90 min after tracer injection and lasted for 30 min. Prior to the PET scan, a low- dose computed tomography scan was performed for attenuation correction. Random and scatter corrections were also applied. Images were reconstructed using Ordered Subsets Expectation Maximization (4 iterations x 16 subsets).

2.4.2 Image analysis

The PET data were reconstructed as 6 frames of 5 minutes and realigned to the first frame to correct for potential head motion. Subsequently, the 6 frames were summed to create one summed image. The individual's T1-weighted structural image was then coregistered to this PET summed image. This MR image was subsequently normalized to the SPM8 T1 template. The same normalization matrix was then applied to the individual's coregistered PET summed image. From the spatially normalized PET images (voxel size 2 x 2 x 2 mm^3), standardized uptake value ratios (SUVR) were calculated in a voxelwise manner with cerebellar grey matter (GM) as reference region. The cerebellar grey matter reference region was defined as areas 91 to 108 of the Automated Anatomical Labelling atlas (AAL) (Tzourio-Mazoyer et al. 2002). The cerebellar reference region was resliced to each individual's normalized PET summed image. In order to exclude most of the white matter (WM) content, it was masked by the normalized and modulated subject-specific GM map, with the threshold for masking set at > 0.3.

Our primary PET outcome measure was the mean SUVR in a composite cortical volume of interest (VOI) ($SUVR_{comp}$). This composite VOI consisted of 5 bilateral cortical regions: frontal (AAL areas 3-10, 13-16, 23-28), parietal (AAL 57-70), anterior cingulate (AAL 31-32), posterior cingulate (AAL 35-36) and lateral temporal (AAL 81-82, 85-90). The composite cortical VOI was resliced to each individual's normalized PET summed image. In order to exclude most of the WM content, it was masked by the normalized and modulated subject-specific GM map, with the threshold for masking set at > 0.3.

While we used $SUVR_{comp}$ as a continuous variable in our primary analysis, we also conducted a secondary analysis where amyloid load was treated as a binary variable and cases were classified as amyloid-positive versus -negative based on a $SUVR_{comp}$ cut-off. Such a binary approach is closer to the way in which Sperling et al. (2011) conceptualized preclinical AD. The $SUVR_{comp}$ cut-off for binary classification was derived from an independent dataset (Vandenberghe et al. 2010) which contained 27 scans from AD patients (mean age 70, SD 7.0) and 15 scans from healthy older controls (HC) (mean age 69, SD 7.6). ^{18}F-flutemetamol scans from the Vandenberghe et al. (2010) study were re-analysed using

the MRI-informed PET analysis method described above. The cut-off was defined based on the statistical distance between the AD group and the HC as described in Vandenberghe et al. (2010). This gave a $SUVR_{comp}$ cut-off equal to 1.38. Note that this cut-off is lower than the cut-off defined by Vandenberghe et al. (2010) or Thurfjell et al. (2014) for a purely PET-based approach, probably due to exclusion of more white matter signal in the MRI-informed method in the amyloid-negative cases. Because of this difference, we also verified our binary case classification using the PET-based method and cut-off from Thurfjell et al. (2014) (cut-off equal to 1.57).

We verified our findings using partial volume corrected (PVC) data. PVC was based on the MRI using the modified Müller-Gärtner method (Müller-Gärtner et al. 1992; Adamczuk et al. 2013). This method makes use of probabilistic segmentation and determines tracer concentration per unit volume of GM. The normalized unmodulated GM and WM segmentations were used to estimate different tissue fractions per voxel. PVC was applied to the normalized PET summed images. The remaining procedures were identical to those outlined above.

2.5 Statistical analysis

2.5.1 Analysis of behavioural data obtained during fMRI

RTs and accuracies (% correct responses) were analysed by means of a four-factor repeated-measures ANOVA, with stimulus modality (2 levels: pictures vs words) and task (2 levels: associative-semantic vs visuoperceptual) as within-subject factors and, as between-subject factors, BDNF (2 levels: codon 66 *met* carriers vs non-carriers) and APOE (2 levels: ε4 carriers vs non-carriers) genotype (Table 3). Pairwise comparisons were performed using Bonferroni post hoc tests.

Table 3

Performance during fMRI experiment

	Reaction time (ms)					Accuracy (% correct)				
BDNF / *APOE*	*met+* ε4+	*met-* ε4+	*met+* ε4-	*met-* ε4-	All groups	*met+* ε4+	*met-* ε4+	*met+* ε4-	*met-* ε4-	All groups
Sem W	2653	2852	2679	2725	2717	88.8	85.5	90.7	89.0	88.8
	(395)	(326)	(300)	(449)	(376)	(7.4)	(4.7)	(4.2)	(9.0)	(7.0)
Sem P	2885	2839	2771	2858	2840	80.2	83.5	82.6	81.3	81.7
	(530)	(332)	(293)	(462)	(417)	(8.7)	(7.9)	(9.5)	(9.0)	(8.7)
Visuo W	2343	2570	2474	2457	2451	81.2	75.7	75.1	80.7	78.5
	(404)	(407)	(381)	(357)	(382)	(10.3)	(15.8)	(16.0)	(15.6)	(14.4)
Visuo P	2633	2765	2534	2647	2636	76.3	71.7	81.2	85.0	79.3
	(611)	(447)	(426)	(382)	(468)	(13.9)	(17.8)	(15.2)	(14.5)	(15.5)

Note: Values represent means and standard deviations. Sem W = associative-semantic task with words; Sem P =

associative-semantic task with pictures; Visuo W = visuoperceptual task with words; Visuo P = visuoperceptual task with pictures.

2.5.2 Whole-brain voxelwise analysis

All voxelwise analyses were performed using SPM8. For each subject, parameter estimates were generated modelling each of the 5 conditions. We then created the following contrast images, averaging across runs:

1. (Associative-semantic task with words + Associative-semantic task with pictures) - (Visuoperceptual task with words + Visuoperceptual task with pictures)
2. Associative-semantic task with words - Visuoperceptual task with words
3. Associative-semantic task with pictures - Visuoperceptual task with pictures
4. (Associative-semantic task with words - Visuoperceptual task with words) - (Associative-semantic task with pictures - Visuoperceptual task with pictures) and inversely
5. (Associative-semantic task with words + Associative-semantic task with pictures) - baseline
6. (Visuoperceptual task with words + Visuoperceptual task with pictures) - baseline
7. Visuoperceptual task with words - baseline
8. Visuoperceptual task with pictures - baseline

The first-level contrast images were then used for second-level whole-brain analysis.

Our primary outcome analysis consisted of a whole-brain voxelwise linear regression analysis with $SUVR_{comp}$ as independent variable, and fMRI response in contrast 1 (main effect of task) as dependent variable. The statistical map was thresholded at a significance threshold of voxel-level $P_{uncorrected} < 0.001$ combined with a cluster-level $P_{corrected} < 0.05$, family-wise error (FWE) corrected for the whole brain volume.

As a secondary outcome analysis, we examined for each of the 10 regions that constitute the composite cortical VOI, the correlation between regional SUVR and the main effect of task (contrast 1) across the whole brain.

Furthermore, we examined whether any significant correlations with amyloid load were found for contrasts 2-8.

As a further secondary outcome analysis, we performed a whole-brain voxel-by-voxel linear regression between SUVR images and fMRI images representing associative-semantic minus visuoperceptual activity (contrast 1) using Biological Parametric Mapping (BPM) (Casanova et al. 2007). The BPM is a toolbox for multimodal image analysis which is based on a voxel-wise use of the SPM's general linear model. This allows comparison of different imaging modalities within voxels.

As a further secondary analysis, we categorized the cases into amyloid- positive versus amyloid-negative and compared the main effect of task between the two groups (contrast 1) using a two-sample *t* test.

We also tested if there was any difference in fMRI response between the four genetic groups by means of a factorial ANOVA with BDNF (2 levels: *met* allele present vs absent) and APOE (2 levels: $\varepsilon 4$ allele present vs absent) as between-subject factors and the main effect of task (contrast 1) as dependent variable.

All whole-brain voxelwise analyses were thresholded at a significance threshold of voxel-level $P_{uncorrected} < 0.001$ combined with a cluster-level $P_{corrected} < 0.05$, FEW corrected for the whole brain volume. In the BPM analysis we used threshold of voxel-level $P_{uncorrected} < 0.001$ combined with cluster size of at least 10 voxels.

2.5.3 Relationship to offline measures of linguistic performance

When our primary analysis revealed clusters of significant correlation between $SUVR_{comp}$ and fMRI response during associative-semantic versus visuoperceptual processing (contrast 1), we examined in further detail whether mean fMRI response in these clusters correlated with a pre-specified set of offline measures of linguistic performance. Clusters of voxels exhibiting a significant correlation between $SUVR_{comp}$ and fMRI response (contrast 1) were extracted using the MarsBaR 0.43 toolbox (http://marsbar.sourceforge.net/). Given the proposed role of the posterior STS in lexical-semantic retrieval (Vandenbulcke et al. 2007), the principal measures that we selected a priori were 1) Reaction times during the confrontation naming task, 2) Reaction times during the lexical decision task, 3) The *b* parameter from the speeded word identification task. For each of these parameters, we performed a stepwise linear regression analysis with this parameter as dependent variable and the independent variables: fMRI response during the associative-semantic minus the visuoperceptual condition (contrast 1), $SUVR_{comp}$, age, education level, BDNF genotype, and APOE genotype. Probability to enter the model was set at $P < 0.05$ with probability to remove set to $P > 0.1$. This analysis was performed outside SPM in a VOI-based manner using STATISTICA 11 (http://www.statsoft.com/) as SPM software does not include stepwise linear regression.

In an additional, binary approach, we examined which of these neurolinguistic measures differed between the amyloid-positive and the amyloid-negative class (two-sample *t* test).

3 Results

3.1 Analysis of behavioural scores during fMRI

The main effect of task was significant: subjects responded more accurately during the associative-semantic conditions than during the visuoperceptual conditions ($F(1,52) = 17.4$, $P = 0.0001$), albeit with longer RTs ($F(1,52) = 24.9$, $P = 0.000007$) (Table 3). The main effect of modality was also significant: subjects responded more slowly ($F(1,52) = 21.3$, $P = 0.00003$) and less accurately ($F(1,52) = 5.7$, $P = 0.02$) for pictures than for words (Table 3). The interaction between task and modality was significant ($F(1,52) = 11$, $P = 0.002$): the associative-semantic task was performed more accurately with words than with pictures ($P = 0.00008$), while there was no difference between words and pictures for the visuoperceptual task ($P = 1$). There was no main effect of BDNF and APOE genotypes on accuracy or RT ($P > 0.2$) (Table 3). The three-way interaction between task, modality and APOE genotype was significant for accuracies ($F(1,52) = 8.2$, $P = 0.006$) (Table 3). According to a posthoc analysis, APOE $\varepsilon 4$ non-carriers performed the associative-semantic task more accurately with words than with pictures ($P = 0.0006$), while there was no difference between the two input-modalities for the visuoperceptual task ($P = 0.35$). No such difference was seen in the APOE $\varepsilon 4$ carriers ($P = 0.23$). We did not find any significant interactions for reaction times ($P > 0.05$).

3.2 Whole-brain voxelwise analysis

3.2.1 Univariate contrast between fMRI conditions

The contrast between the associative-semantic minus the visuoperceptual conditions (main effect of task, contrast 1) revealed a distributed semantic network consistent with previous findings (Vandenberghe et al. 1996; Vandenbulcke et al. 2007; Nelissen et al. 2007) (Fig.

2A). The interaction between task and input modality (contrast 4) revealed word-specific activation during the semantic compared to the visuoperceptual task in left STS, extending from posterior to more anterior portions of the STS (cluster peak coordinates -66, -36, 9, extent (ext) = 113 voxels, cluster-level $P_{corrected}$ = 0.0001) (Fig. 2B). Picture-specific semantic activation (inverse of contrast 4) occurred bilaterally in ventral occipitotemporal cortex extending to superior occipital gyrus (right cluster peak coordinates 33, -45, -21, ext = 1756 voxels, cluster-level $P_{corrected} < 0.0001$ and left cluster peak coordinates -39, -51, -15, ext = 1286 voxels, cluster-level $P_{corrected} < 0.0001$) and in right inferior frontal gyrus (cluster peak coordinates 48, 12, 27, ext = 141 voxels, cluster-level $P_{corrected} < 0.0001$) (Fig. 2C).

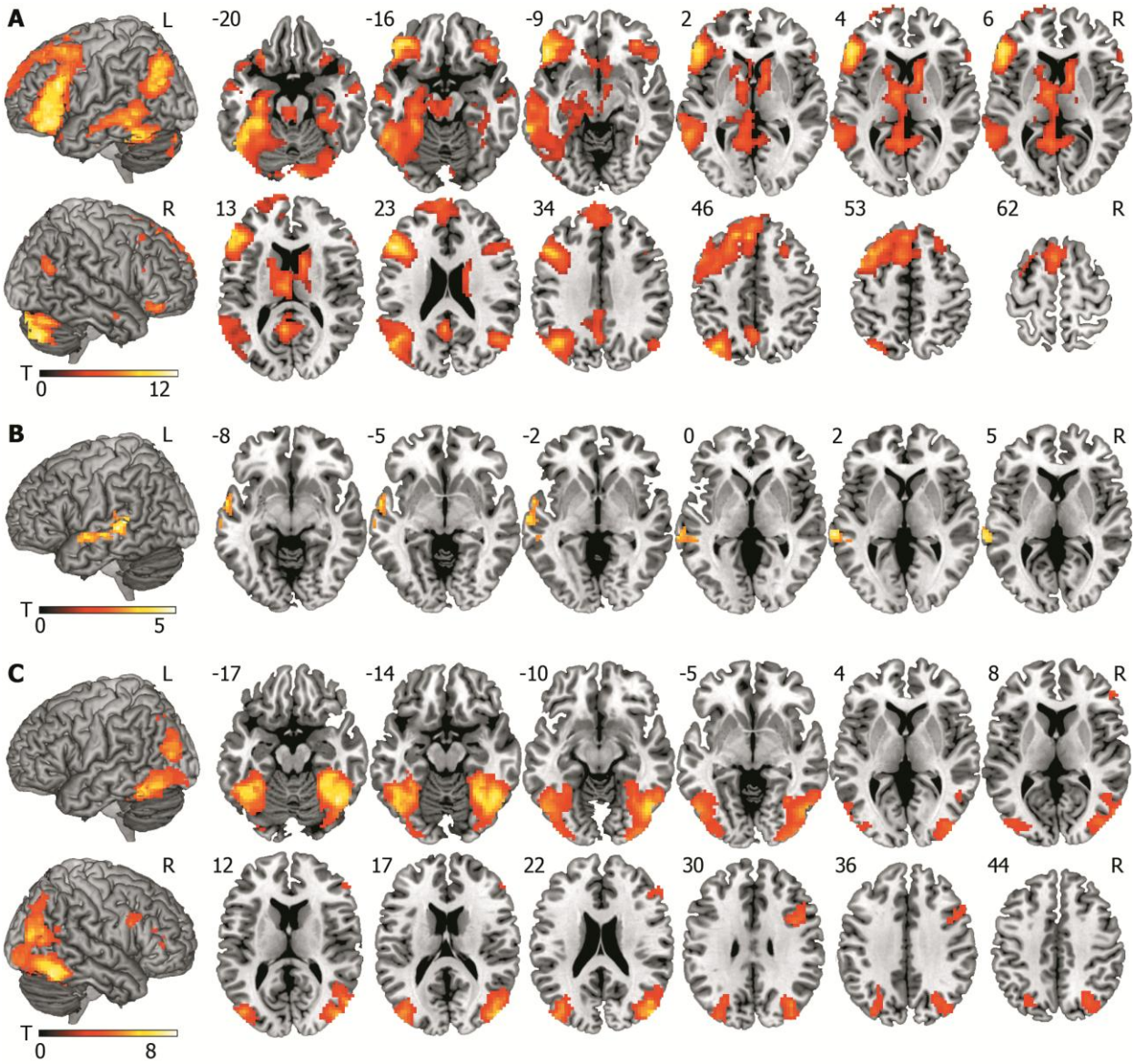

Figure 2: **(A)** Main effect of associative-semantic task minus visuopercetual task (contrast 1). **(B)** Interaction effect of task and modality: effect of semantic words (contrast 4, i.e. (associative-semantic task with words - visuoperceptual task with words) - (associative-semantic task with pictures - visuoperceptual task with pictures)). **(C)** Interaction effect of task and modality: effect of semantic pictures (inverse of contrast 4, i.e. (associative-semantic task with pictures - visuoperceptual task with pictures) - (associative-semantic task with words - visuoperceptual task with words)). Shown activations are significant at the threshold of voxel-level $P_{uncorrected}$ = 0.001 combined with cluster-level $P_{corrected}$ = 0.05. The colour scales indicate the *T*-values for the contrasts. MNI coordinates are indicated in the left upper corner and orientation of the brain in the right upper corner.

3.2.2 Linear regression between fMRI response and amyloid load

In a whole-brain analysis, the posterior third of the left middle temporal gyrus (MTG) (Fig. 3A) exhibited a significant positive correlation between fMRI response during the associative-semantic versus the visuoperceptual task (contrast 1) and $SUVR_{comp}$: activity levels were higher with a higher amyloid load (-57, -45, 9, ext = 64 voxels, cluster-level $P_{corrected}$ = 0.006) (Fig. 3A-E). No other regions showed a correlation, even when we lowered the significance threshold to cluster-level $P_{corrected} < 0.25$. The MTG belonged to the amodal network, as evidenced by the conjunction analysis of contrast 2 and 3 (Fig. 4A, B, C).

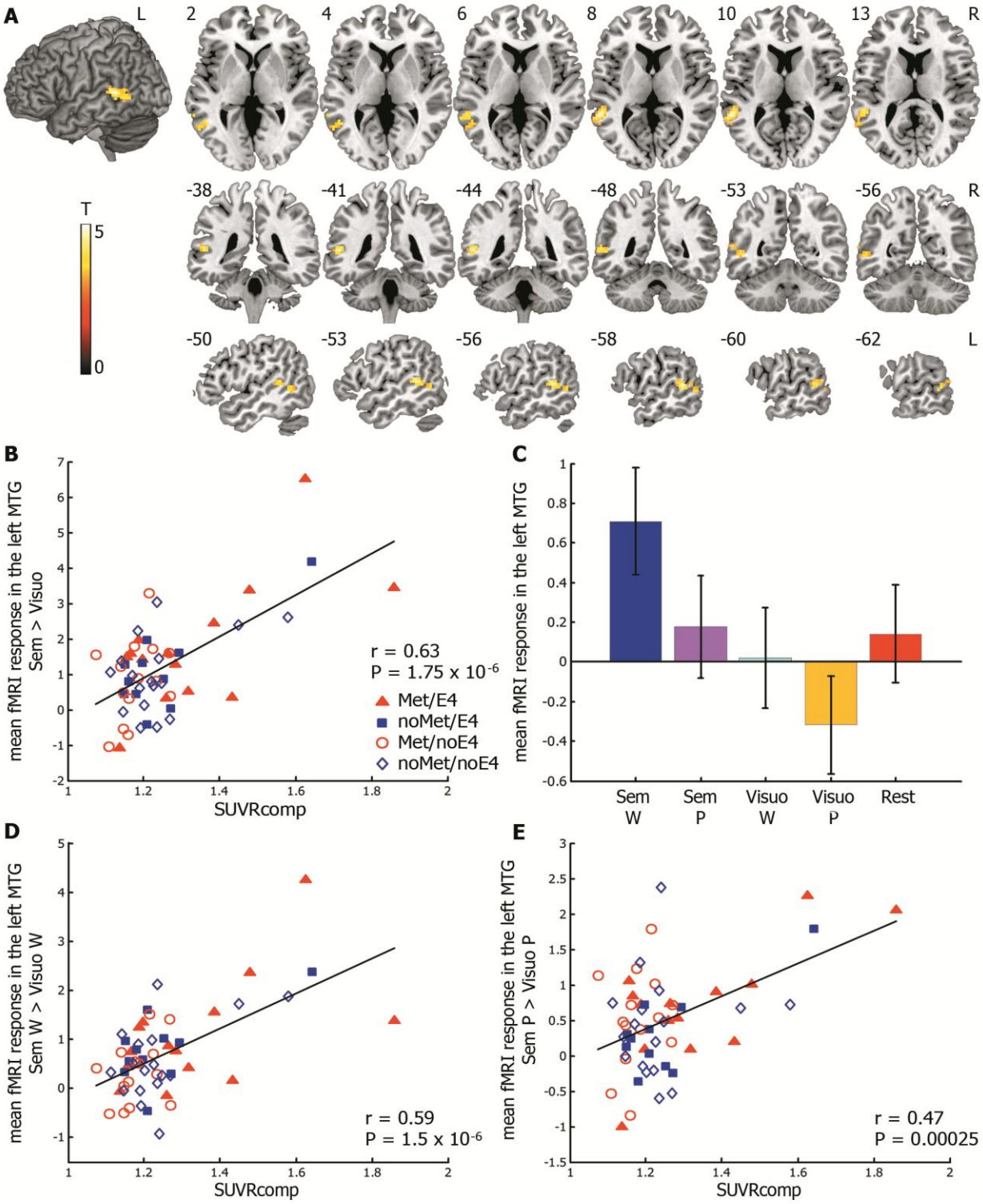

Figure 3: (A) Area in the left posterior MTG of significant correlation between $SUVR_{comp}$ and fMRI response during associative-semantic minus visuoperceptual condition (contrast 1) (cluster peak -57, -45, 9, ext = 64 voxels, cluster-level $P_{corrected} = 0.006$). The colour scale indicates the *T*-values. MNI coordinates are indicated in the left upper corner and orientation of the brain in the right upper corner. **(B)** Plot of correlation between $SUVR_{comp}$ (X axis) and mean fMRI contrast values in the left MTG VOI during associative-semantic minus visuoperceptual condition (contrast 1) (Y axis) ($r = 0.63$, $P < 0.0001$). **(C)** Bar plot depicting mean fMRI contrast values (Y axis) in the left posterior MTG during each condition (X axis). Error bars: standard error; Sem W: associative-semantic task with words (*blue*); Sem P: associative-semantic task with pictures (*purple*); Visuo W: visuoperceptual task with words (*cyan*); Visuo P: visuoperceptual task with pictures (*yellow*); Rest: resting baseline condition (*red*). **(D)** Correlation of $SUVR_{comp}$ (X axis) with mean fMRI contrast values during associative- semantic word processing (contrast 2) in the left MTG VOI (Y axis) ($r = 0.59$, $P < 0.0001$). **(E)** Correlation of $SUVR_{comp}$ (X axis) with mean fMRI contrast values during associative-semantic picture processing (contrast 3) in the left MTG VOI (Y axis) ($r = 0.47$, $P = 0.00025$). Black lines: linear regressions; *red triangles*: BDNF *met*+ve/APOE ε4 +ve; *blue squares*: BDNF *met*-ve/APOE ε4 +ve; *red circles*: BDNF *met*+ve/APOE ε4 -ve; *blue diamonds*: BDNF *met*-ve/APOE ε4 -ve.

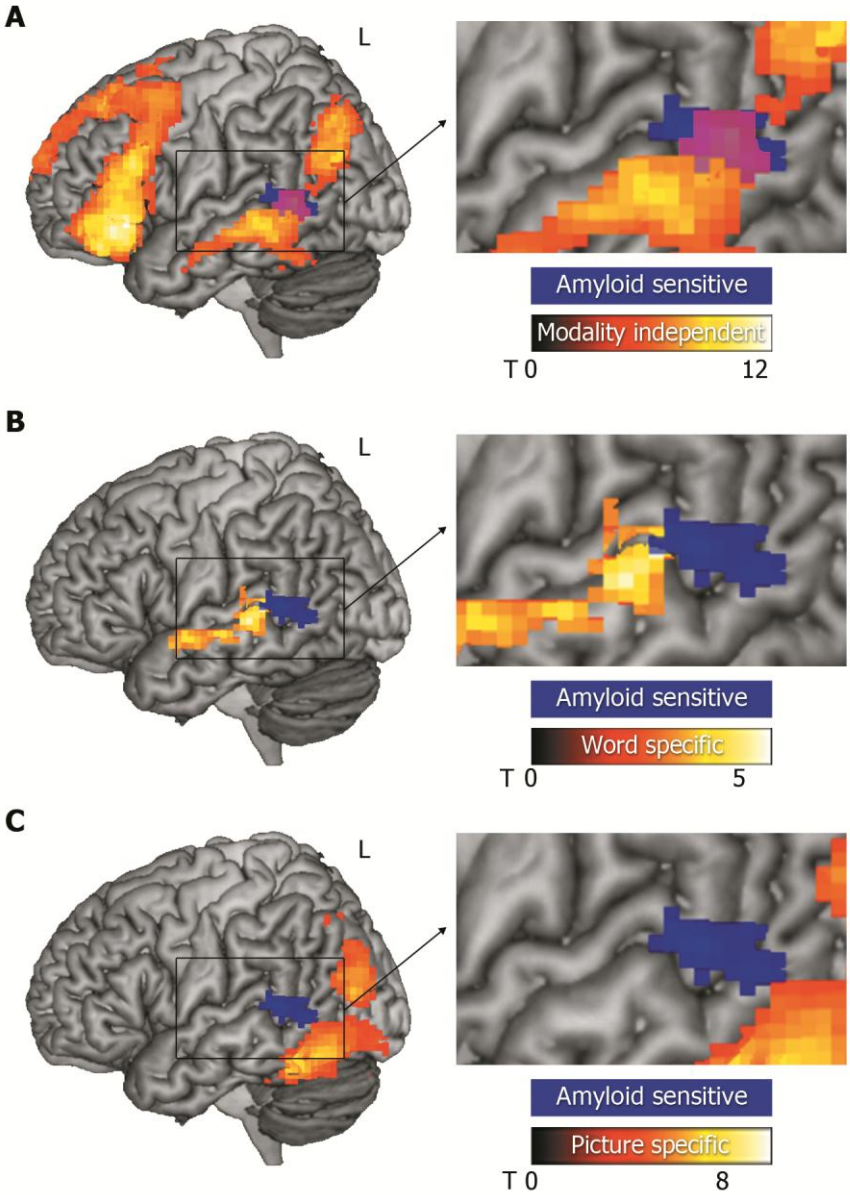

Figure 4: (A) Functional left MTG VOI belongs to the amodal associative-semantic network (conjunction of contrast 2 and 3) (MTG cluster pick -63, -45, 3, ext = 51 voxels, voxel-level $P_{corrected} = 0.000002$). Overlap is shown in *purple*. **(B)** Left MTG VOI did not belong to the word specific associative-semantic areas (contrast 4) (voxel-level $P_{corrected} > 0.16$) and **(C)** neither to the picture specific semantic areas (inverse of contrast 4) (voxel-level $P_{corrected} > 0.18$). The left MTG VOI is shown in *blue*. The hot colour scales indicate the *T*-values of associative-semantic network (A), word specific associative-semantic regions (B), and picture specific associative-semantic regions (C). Orientation of the brain is indicated in the right upper corner. All *P*-values were FWE corrected for multiple comparisons in a small volume.

When we restricted the contrast between the associative-semantic and the visuoperceptual task to the words (contrast 2) and examined the correlation with amyloid load in the whole-brain analysis, $SUVR_{comp}$ correlated positively with fMRI response during the associative-semantic minus visuoperceptual control condition for words in the same region (-60, -48, 9, ext = 49 voxels, cluster-level $P_{corrected}$ = 0.02). For pictures, there was no correlation (contrast 3) (cluster-level $P_{corrected} > 0.6$). No other regions showed a correlation, even when we lowered the significance threshold to cluster-level $P_{corrected} < 0.10$. Neither were any correlations with $SUVR_{comp}$ found for contrast 4-8.

Analysis of partial volume corrected data confirmed these results. PVC $SUVR_{comp}$ positively correlated with fMRI response during the associative-semantic minus the visuoperceptual condition (contrast 1) in the posterior third of the left MTG (-54, -39, 12, ext = 87 voxels, cluster-level $P_{corrected}$ = 0.001). Analysis restricted only to the word conditions showed that $SUVR_{comp}$ correlated positively with fMRI response during the associative-semantic minus visuoperceptual control condition for words (contrast 2) in the same region (-54, -36, 9, ext = 45 voxels, cluster-level $P_{corrected}$ = 0.028). No correlation was found between $SUVR_{comp}$ and the fMRI response during the associative-semantic minus visuoperceptual condition when only pictures were used (contrast 3) (cluster-level $P_{corrected} > 0.07$).

Among the regions which constituted the composite cortical VOI, average SUVR in each of the regions besides the left and right anterior cingulate and left lateral frontal region contributed to the correlation of fMRI response during contrast 1 and $SUVR_{comp}$ (cluster-level $P_{corrected} < 0.038$).

Biological parametric mapping indicated a significant correlation within-voxels between fMRI activity and SUVR in the posterior left MTG (cluster peak coordinates -60, -54, 12, ext = 18 voxels, voxel-level $P_{uncorrected} = 0.0001$, $Z = 3.65$, $r = 0.50$).

3.2.3 Binary classification

We evaluated whether similar results would be obtained had we used a binary approach: amyloid-positive versus amyloid-negative group (Fig. 5). Eight subjects (14%) were classified as positive (Fig. 5). fMRI performance parameters did not differ between the amyloid-positive and the amyloid-negative group (Table 4). In a whole-brain voxelwise analysis, the amyloid-positive group exhibited a higher fMRI response compared to the amyloid-negative group during the associative-semantic minus visuoperceptual conditions (contrast 1) in the posterior third of the MTG (-54, -42, 9, ext = 55 voxels, cluster-level $P_{corrected}$ = 0.013) (Fig. 5B red cluster). This was also true for the contrast between the associative-semantic minus visuoperceptual task presented as words (contrast 2) (-57, -45, 6, ext = 59 voxels, cluster-level $P_{corrected}$ = 0.008) (Fig. 5B green cluster). Overlap between clusters is shown in dark orange (Fig. 5B). We did not find any significant differences elsewhere and neither did we find any significant between-group differences for other contrasts. When we applied the Thurfjell et al. (2014) method and cut-off for binary classification, 4 cases were positive. The between-group differences remained essentially the same: the amyloid-positive group had higher fMRI response compared to the amyloid-negative group during the associative-semantic versus visuoperceptual condition (-60, -48, 9, ext = 54 voxels, cluster-level $P_{corrected}$ = 0.014).

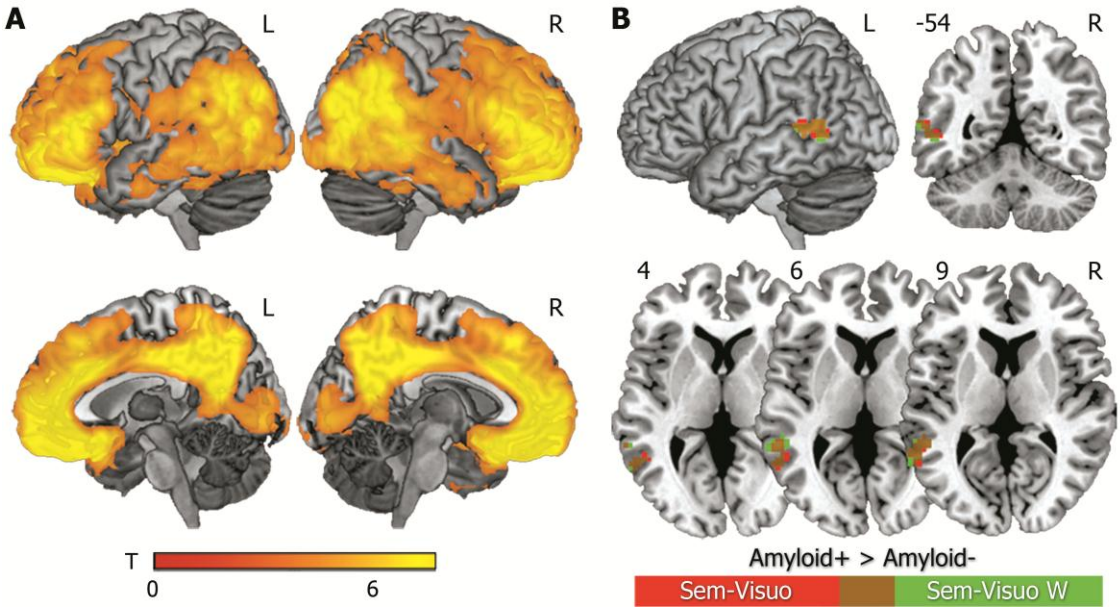

Figure 5: (A) Older healthy amyloid-positive subjects had higher amyloid deposition compared to amyloid-negative subjects in typical regions for increased amyloid load (precuneus, anterior and posterior cingulate, lateral prefrontal, lateral parietal, and lateral temporal, ext = 39779 voxels, cluster-level $P_{corrected}$<0.0001). The hot colour scale indicates the *T*-values for the differences. **(B)** Older healthy amyloid-positive subjects had increased fMRI response compared to amyloid-negative subjects during the associative-semantic minus visuoperceptual conditions (contrast 1) in the posterior third of the MTG (-54, -42, 9, ext = 55 voxels, cluster-level $P_{corrected}$ = 0.013; in *red*), and during the associative-semantic minus visuoperceptual task presented as words (contrast 2) also in the MTG (-57, -45, 6, ext = 59 voxels, cluster- level $P_{corrected}$ = 0.008; in *green*). Overlap between clusters is shown in *dark orange*. Results are thresholded at voxel-level $P_{uncorrected}$ = 0.001 combined with cluster-level $P_{corrected}$ = 0.05. MNI coordinates are indicated in the left upper corner and orientation of the brain in the right upper corner.

3.3 Genotype effect on fMRI response and relationship between fMRI response and SUVR

APOE and BDNF genotype did not affect the activity patterns during the associative-semantic versus visuoperceptual conditions (cluster-level $P_{corrected}$ > 0.8). Nor was there an effect of BDNF or APOE genotype on the correlation between mean fMRI response in the left posterior MTG (contrast 1) and $SUVR_{comp}$ (P>0.1) (BDNF *met* carriers r = 0.64, P = 0.0002; BDNF non-carriers r = 0.61, P = 0.0005; APOE ε4 carriers r = 0.71, P = 0.00006; APOE ε4 non-carriers r = 0.40, P = 0.03) (Fig. 6).

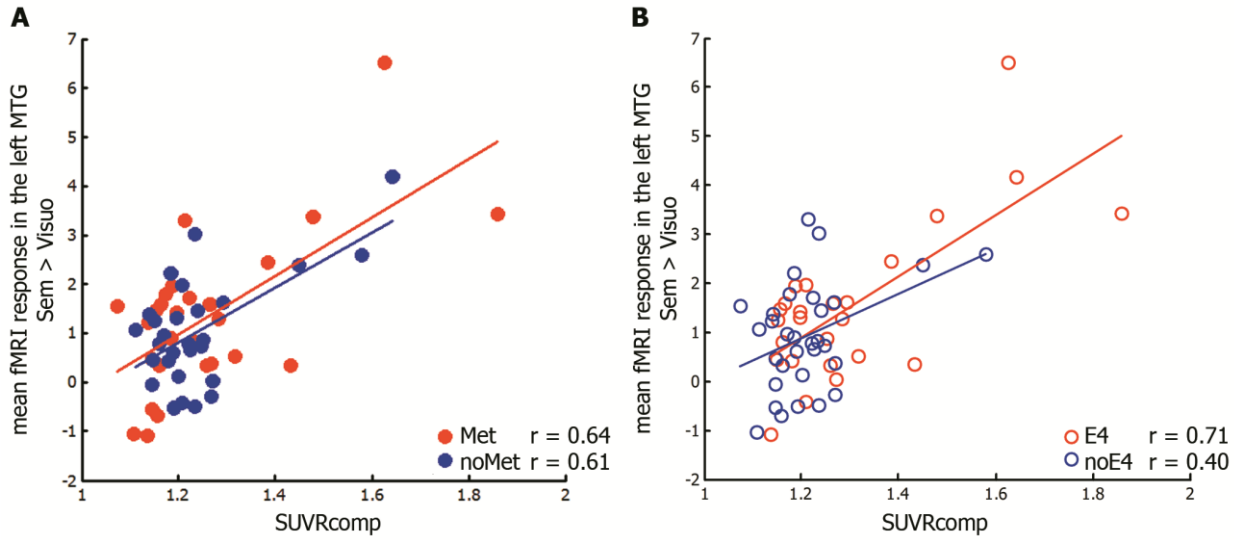

Figure 6: (A) The difference between correlations for BDNF *met* carriers (*red full circles*) and non-carriers (*blue full circles*) (P = 0.86). **(B)** The difference between correlations for APOE ε4 carriers (*red empty circles*) and non-carriers (*blue empty circles*) (P = 0.11). Y axes: mean fMRI response during the associative-semantic minus the visuoperceptual condition (contrast 1) in functional left MTG VOI. X axes: $SUVR_{comp}$. Lines show linear regressions.

3.4 Relationship with offline language measures

According to a stepwise regression analysis, variance in RT during the confrontation naming task was partly explained by $SUVR_{comp}$ (r = 0.27, P = 0.04), rather than fMRI response (contrast 1; P = 0.62), age (P = 0.34), education (P = 0.57), BDNF (P = 0.21), or APOE status (P = 0.42) (Fig. 7).

Response latencies during confrontation naming were longer in the amyloid- positive compared to the amyloid-negative group (P = 0.047) (Table 4). There were no differences for any of the other experimental language tests and neither did the conventional neuropsychological test scores differ between the amyloid-positive and -negative class (Table 4).

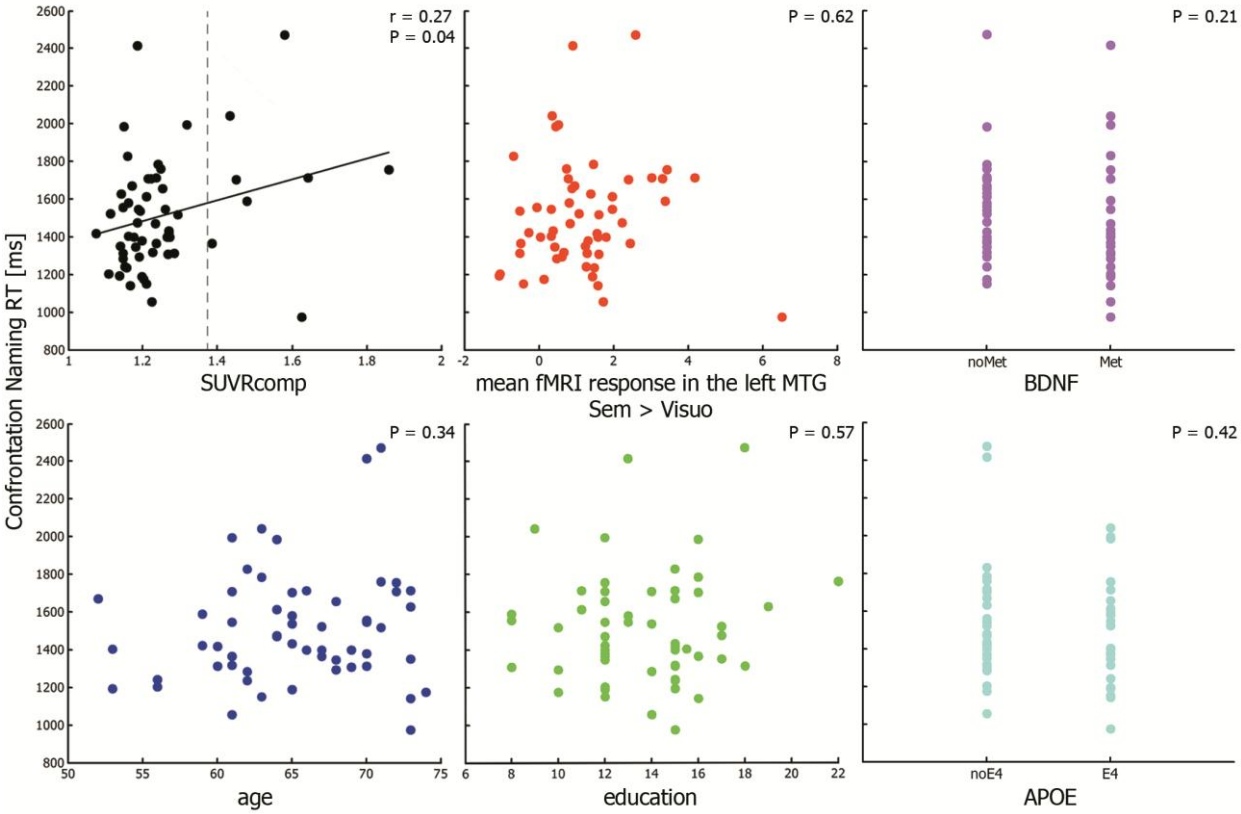

Figure 7: Results of a stepwise regression analysis. RT during the confrontation naming task (Y axis) was best predicted by the $SUVR_{comp}$ (*black circles*) (r = 0.27, P = 0.04), and not by fMRI response from contrast 1 (*red circles*) (P = 0.62), age (*blue circles*) (P = 0.34), education (*green circles*) (P = 0.57), BDNF (*purple circles*) (P = 0.21), or APOE (*cyan circles*) (P = 0.42) status. X axis represents values of the predictor variables. Grey dashed line = $SUVR_{comp}$ cut-off of 1.38.

Table 4

Differences between amyloid-positive and -negative subjects

	Age (yr)	Gender (M/F)	Education (yr)	MMSE (/30)	AVTL TL (/75)	AVLT DR (/15)	BNT (/60)	AVF (# words)	LVF (# words)	RPM (/60)
Amyloid+	67.9 (5.2)	3/5	13.1 (3.5)	28.5 (0.9)	44.1 (6.8)	10.5 (1.8)	52.8 (4.1)	18.4 (4.2)	30.0 (13.8)	39.3 (12.1)
Amyloid-	64.8 (5.5)	28/20	13.8 (2.7)	29.1 (0.9)	50.0 (9.7)	10.8 (2.8)	53.3 (4.9)	20.8 (5.1)	34.5 (9.7)	43.7 (7.7)
P	0.14	0.27	0.55	0.10	0.10	0.81	0.78	0.21	0.26	0.17

	BDNF	APOE	Conf naming		Lexical decision		Speeded id W		
	met+/*met*-	ε4+/ε4-	RT (ms)	Accu (%)	RT (ms)	Accu (A')	*a* (ms)	*b* (ms)	*c* (ms)
Amyloid+	5/3	6/2	2203 (441)	92.3 (0.0)	1109 (322)	98.0 (0.0)	21.3 (9.9)	21.4 (10.9)	98.6 (1.3)
Amyloid-	23/25	19/29	1978 (258)	91.9 (0.1)	1106 (231)	98.9 (0.0)	22.4 (13.4)	20.7 (10.8)	99.1 (1.5)
P	0.45	0.06	**0.047**	0.84	0.97	0.11	0.83	0.86	0.42

	Sem W		Sem P		Visuo W		Visuo P	
	RT (ms)	Accu (%)	RT (ms)	Accu (%)	RT (ms)	Accu (%)	RT (ms)	Accu (%)
Amyloid+	2885 (416)	89.4 (4.0)	2883 (564)	83.5 (9.3)	2571 (443)	82.3 (11.0)	2856 (686)	74.8 (15.7)
Amyloid-	2689 (367)	88.7 (7.4)	2833 (395)	81.4 (8.7)	2431 (372)	77.9 (14.9)	2599 (420)	80.1 (15.5)
P	0.17	0.79	0.76	0.53	0.34	0.43	0.15	0.38

Note: Values represent means and standard deviations. Gender, APOE, and BDNF genotypes are expressed in number of individuals. Abbreviations are explained in Table 1, 2, and 3. *P*-values represent significance for two-sample *t* test or *chi* square test (gender, APOE, BDNF).

4 Discussion

In cognitively intact older adults, a higher amyloid burden was associated with subclinical alterations of the network for language and associative-semantic processing. Activity in left posterior middle temporal gyrus was higher with a higher amyloid load (Fig. 3A, B). Higher amyloid levels were correlated with slower confrontation naming (Fig. 7). Our posterior temporal findings are based on a whole-brain search without prior restriction of the search volume. They were in agreement with our a priori hypothesis about posterior temporal cortex, although the exact location was in the amodal posterior MTG (Fig. 4A) adjacent to the word-specific posterior STS found before in MCI (Vandenbulcke et al. 2007) and AD (Nelissen et al. 2007) patients.

While we used the $SUVR_{comp}$ as a continuous variable for the primary outcome analysis, we also conducted a secondary analysis where amyloid load was treated as a binary variable and cases were classified as amyloid-positive versus -negative based on a $SUVR_{comp}$ cut-off. Such a binary approach is closer to the way in which Sperling et al. (2011) conceptualize preclinical AD. The findings based on a binary approach were entirely in line with the findings obtained with the linear regression approach (Fig. 5).

During the visuoperceptual control conditions subjects engaged in an active comparison of the size-on-the-screen of a picture or a word. It is highly plausible that the meaning of this word or picture is automatically activated to some degree during the visuoperceptual condition too. A lower-level control condition with consonant letter strings or scrambled pictures (Ricci et al. 1999) would have been necessary had we wanted to isolate the regions activated during word and picture processing in the visuoperceptual condition. In any case, we did not find a correlation between amyloid load and the activity pattern during the visuoperceptual control conditions minus fixation baseline. This could suggest that the network underlying activation of word and picture meaning during the visuoperceptual condition is relatively intact in preclinical AD and that the principal changes are at the level of explicit associative-semantic processing.

Our findings are based on observational cross-sectional data, analysed by means of correlational analysis and between-group comparisons. One therefore has to be careful in drawing conclusions about a causal link between the increase in amyloid burden, the increase in left posterior temporal activity, and the decrease in confrontation naming latencies. To adequately resolve this fundamental limitation, one would need to conduct interventional studies. This is difficult since there are no proven amyloid-lowering interventions available. Transcranial magnetic stimulation targeting the left posterior temporal cortex could be an option to examine how altering activity within a subject affects naming latencies and whether this depends on amyloid load.

We also observed right-hemispheric inferior frontal activation during the associative-semantic versus the visuoperceptual task (Fig. 2A), and this was particularly pronounced for the pictures (Fig. 2C). The right inferior frontal activation could be related to the older age range of our individuals, in line with the Hemispheric Asymmetry Reduction in Older Adults model (Cabeza 2002; Cabeza et al. 2005). However, one would need fMRI data over a wider age range including also young adults to confirm this. In any case, no increase in right-hemispheric activation was found as a consequence of increasing amyloid load in our dataset, contrary to our original hypothesis (Nelissen et al. 2007).

Previous studies have investigated changes in task-related fMRI in AD principally within the episodic memory domain. AD patients consistently show lower hippocampal activation in episodic memory encoding tasks in comparison to controls and/or MCI subjects

(Small et al. 1999; Machulda et al. 2003; Sperling et al. 2003; Golby et al. 2005; Celone et al. 2006; Sperling 2007). Subjects with late MCI also have decreased hippocampal activity during episodic memory encoding (Machulda et al. 2003; Johnson et al. 2006a) while subjects with early MCI compared to controls show an increase in hippocampal activity during memory encoding (Dickerson et al. 2005; Johnson et al. 2006b). Young healthy presenilin 1 mutation carriers destined for early-onset AD exhibit higher activity in the hippocampal formation in comparison to the non-carrier controls (Mondadori et al. 2006; Reiman et al. 2012). Subjects with a higher risk for AD due to family history and APOE ε4 carrier status also have higher hippocampal activation during encoding compared to non-carrier controls (Fleisher et al. 2005). These studies led to a model where the direction of functional changes in medial temporal cortex is stage-dependent: in the preclinical AD stage and the early MCI stage, activity during memory encoding in the hippocampus is increased compared to controls, while in the late MCI and the clinically probable AD stage activity is decreased compared to controls. Our findings indicate that a similar sequence may occur in the language domain in left posterior temporal cortex. The current data show increased activity during associative-semantic processing in preclinical AD according to the National Institute on Aging and Alzheimer's Association criteria (Sperling et al. 2011). In a previous study in amnestic MCI, activity in left posterior STS was decreased and correlated with the speed of written word identification (Vandenbulcke et al. 2007). In clinically probable AD, the same region also showed lower activity levels (Nelissen et al. 2007). Our study is the first to report an increase in left posterior temporal cortex in a stage that has been referred to as preclinical AD (Fig. 3), similarly to what has been described in the hippocampal formation for episodic memory (Sperling 2007). Taken together, this series of studies may suggest a similar sequence of increased activity in posterior temporal cortex followed by activity decreases as Alzeimer's disease progresses to the clinical stages.

Initial functional imaging studies of language and semantic memory in clinically probable AD have emphasized prefrontal increases which correlated positively with task performance (Becker et al. 1996; Saykin et al. 1999; Grady et al. 2003). These AD-related prefrontal increases generalized across episodic and semantic memory tasks (Grady et al. 2003) and presumably reflect general adaptive strategic processes (Becker et al. 1996; Grady et al. 2003). A series of studies revealed functional changes also in temporal cortex, most notably left inferior temporal cortex (Grossman et al. 2003a, 2003b), left and right middle temporal gyrus (Grossman et al. 2003a, 2003b, Seidenberg et al. 2009) and left posterior superior temporal sulcus (Nelissen et al. 2007; Vandenbulcke et al. 2007). Functional differentiation exists within left temporal cortex even within nearby areas. For instance, the posterior third of the left STS is activated during semantic processing specifically for words (Vandenberghe et al. 1996; Vandenbulcke et al. 2007). It has been principally implicated in lexical-semantic (Vandenbulcke et al. 2007) or lexical-phonological retrieval (Binder et al. 2000; Price and Mechelli 2005). In contrast, an adjacent more inferior region, the posterior third of the left MTG, is activated during semantic processing for both words and pictures (Fig. 4A versus B and C, Fig. 3D-E). The left posterior middle temporal gyrus is one of the most consistent hubs in the associative-semantic network (Buckner et al. 2005; Vandenberghe et al. 2013a). It has been implicated in amodal semantic processing (Vandenberghe et al. 1996; Vandenbulcke et al. 2007) as well as in semantic control (Whitney et al. 2011, 2012). In the current study the correlation principally occurred within the amodal posterior MTG region rather than the word-specific STS (Fig. 3A, Fig. 4A). Our findings can be readily integrated in current hypotheses that attribute to posterior MTG a role in cognitive control: regions involved in semantic control may be the prime candidates for compensatory processes in response to increases in amyloid load. Increased

amyloid burden in cortical areas may hamper normal neuronal functioning due to its neurotoxic effects. In order to cope with such functional changes at the neuronal level, demands for cognitive control may increase and this may account for the increase in MTG activity levels. Cognitively normal older persons may have increased Aβ levels yet intact neuropsychological performance (Driscoll et al. 2006; Aizenstein et al. 2008), possibly due to ongoing compensatory processes. As the disease advances, mechanisms responsible for maintaining constant level of increased activation may become exhausted, resulting in the first cognitive symptoms. Thus early word finding difficulties in the course of AD might arise due to failure of semantic control processes, followed by a gradual activity decrease in other language areas, e.g. areas directly involved in word processing like posterior STS.

We did not find any effect of genetic polymorphisms of APOE or BDNF on the language network in our cohort. In AD, APOE ε4 status has been associated more closely with episodic memory deficits than with language symptoms (Lehtovirta et al. 1996; Rasmusson et al. 1996; Mendez 2012; Mez et al. 2013). Healthy older controls with a family history of Alzeimer's disease and at least one APOE ε4 allele, have increased fMRI activation during a semantic memory task (famous versus unfamiliar names) in bilateral temporoparietal areas, posterior cingulate and precuneus, posterior middle and superior temporal regions, and left hippocampal complex (Woodard et al. 2009). It is not that we did not find any effect of APOE. As reported before, APOE genotype exerted an effect on the amyloid burden in our cohort: a higher amyloid load in APOE ε4 carriers was present in posterior cingulate, a region outside the network that our paradigm is activating (Adamczuk et al. 2013).

As of yet, the relationship between BDNF and language has been principally studied during development and early adulthood (Freundlieb et al. 2012; Simmons et al. 2010; Li and Bartlett 2012) and in schizophrenia (Kebir et al. 2009). Contrary to our hypothesis, the regression between fMRI response and amyloid load was not influenced by BDNF status. In the same cohort we previously reported that BDNF exerted a direct effect on amyloid load in interaction with APOE: BDNF *met* carriers had increased levels of Aβ in typical regions of predilection in comparison to the BDNF *met* non-carriers with APOE ε4 (Adamczuk et al. 2013). In summary, contrary to our prediction, the effect of BDNF in our cohort is situated at the level of amyloid aggregation rather than at the level of fMRI response.

Our findings highlight the critical role of left posterior temporal cortex in AD-related processes. Changes in left posterior superior temporal sulcus lead to lexical-semantic retrieval deficits which may explain the word finding difficulties in clinical AD (Nelissen et al. 2007) and the subclinical slowing in word identification speed in MCI (Vandenbulcke et al. 2007). The changes we observed in this study in the posterior middle temporal gyrus may reflect higher demands for semantic control in those subjects who are cognitively intact despite a high amyloid burden.

To conclude, our cross-sectional data indicate that a higher amyloid load in cognitively intact individuals has functional consequences for the network mediating language and associative-semantic processing. The converging evidence obtained in cognitively intact older adults, amnestic MCI and AD may suggest a sequence of events similar to that proposed for the hippocampal formation in episodic memory. The initial compensatory role of increased neuronal activity may precede later deterioration.

5 Funding

This work was supported by the Foundation for Alzheimer Research SAO-FRMA (09013, 11020, 13007); Research Foundation Flanders (G.0660.09); KU Leuven (OT/08/056, OT/12/097); IWT VIND; IWT TGO BioAdapt AD; Belspo IAP (P7/11); Research Foundation Flanders senior clinical investigator grant to R.V. and K.V.L.; and Research Foundation Flanders doctoral fellowship to K.A. ^{18}F-flutemetamol was provided by GE Healthcare free of charge for this academic investigator-driven trial.

6 Acknowledgements

We would like to thank the staff of Nuclear Medicine, Radiology, and the Memory Clinic at the University Hospitals Leuven, and the staff of the Genetic Service Facility at the University of Antwerp - VIB Department of Molecular Genetics.

References

Adamczuk K, De Weer AS, Nelissen N, Chen K, Sleegers K, Bettens K, Van Broeckhoven C, Vandenbulcke M, Thiyyagura P, Dupont P et al. 2013. Polymorphism of Brain Derived Neurotrophic Factor influences β amyloid load in cognitively intact Apolipoprotein E ε4 carriers. Neuroimage Clin. 2:512-520.

Aizenstein HJ, Nebes RD, Saxton JA, Price JC, Mathis CA, Tsopelas ND, Ziolko SK, James JA, Snitz BE, Houck PR, Bi W, Cohen AD, Lopresti BJ, DeKosky ST, Halligan EM, Klunk WE. 2008. Frequent amyloid deposition without significant cognitive impairment among the elderly. Arch Neurol. 65:1509-1517.

Apostolova LG, Lu P, Rogers S, Dutton RA, Hayashi KM, Toga AW, Cummings JL, Thompson PM. 2008. 3D mapping of language networks in clinical and pre-clinical Alzheimer's disease. Brain Lang. 104:33-41.

Arendt T, Schindler C, Brückner MK, Eschrich K, Bigl V, Zedlick D, Marcova L. 1997. Plastic neuronal remodeling is impaired in patients with Alzheimer's disease carrying apolipoprotein epsilon 4 allele. J Neurosci. 17:516-529.

Bastiaanse R, Bosje M, Visch-Brink E. 1995. Psycholinguïstische testbatterij voor de taalverwerking van Afasiepatiënten (PALPA). Hove (UK): Lawrence Erlbaum Associates.

Bayles KA, Tomoeda CK. 1983. Confrontation naming impairment in dementia. Brain Lang. 19:98-114.

Becker JT, Mintun MA, Aleva K, Wiseman MB, Nichols T, DeKosky ST. 1996. Compensatory reallocation of brain resources supporting verbal episodic memory in Alzheimer's disease. Neurology. 46:692-700.

Binder JR, Frost JA, Hammeke TA, Bellgowan PS, Springer JA, Kaufman JN, Possing ET. 2000. Human temporal lobe activation by speech and nonspeech sounds. Cereb Cortex. 10:512-528.

Buckner RL, Snyder AZ, Shannon BJ, LaRossa G, Sachs R, Fotenos AF, Sheline YI, Klunk WE, Mathis CA, Morris JC, Mintun MA. 2005. Molecular, structural, and functional characterization of Alzheimer's disease: evidence for a relationship between default activity, amyloid, and memory. J Neurosci. 25:7709-7717.

Cabeza R. 2002. Hemispheric asymmetry reduction in older adults: the HAROLD model. Psychol Aging. 17:85-100.

Cabeza R, Nyberg L, Park DC. 2005. Cognitive Neuroscience of Aging. New York (New York): Oxford University Press.

Casanova R, Srikanth R, Baer A, Laurienti PJ, Burdette JH, Hayasaka S, Flowers L, Wood F, Maldjian JA. 2007. Biological parametric mapping: A statistical toolbox for multimodality brain image analysis. Neuroimage. 34:137-143.

Celone KA, Calhoun VD, Dickerson BC, Atri A, Chua EF, Miller SL, DePeau K, Rentz DM, Selkoe DJ, Blacker D, Albert MS, Sperling RA. 2006. Alterations in memory networks in mild cognitive impairment and Alzheimer's disease: an independent component analysis. J Neurosci. 26:10222-10231.

Chertkow H, Bub D. 1990. Semantic memory loss in dementia of Alzheimer's type. What do various measures measure? Brain. 113:397-417.

Chételat G, La Joie R, Villain N, Perrotin A, de La Sayette V, Eustache F, Vandenberghe R. 2013. Amyloid imaging in cognitively normal individuals, at-risk populations and preclinical Alzheimer's disease. Neuroimage Clin. 2:356-365.

Chételat G, Villemagne VL, Villain N, Jones G, Ellis KA, Ames D, Martins RN, Masters CL, Rowe CC. 2012. Accelerated cortical atrophy in cognitively normal elderly with high β-amyloid deposition. Neurology. 78:477-484.

Clark CM, Pontecorvo MJ, Beach TG, Bedell BJ, Coleman RE, Doraiswamy PM, Fleisher AS, Reiman EM, Sabbagh MN, Sadowsky CH, Schneider JA, Arora A, Carpenter AP, Flitter ML, Joshi AD, Krautkramer MJ, Lu M, Mintun MA, Skovronsky DM. 2012. Cerebral PET with florobetapir compared with neuropathology at autopsy for detection of neuritic amyloid-β plaques: a prospective cohort study. Lancet Neurol. 11:669-678.

Clark CM, Schneider JA, Bedell BJ, Beach TG, Bilker WB, Mintun MA, Pontecorvo MJ, Hefti F, Carpenter AP, Flitter ML, Krautkramer MJ, Kung HF, Coleman RE, Doraiswamy PM, Fleisher AS, Sabbagh MN, Sadowsky CH, Reiman EP, Reiman PEM, Zehntner SP, Skovronsky DM. 2011. Use of florobetapir-PET for imaging beta-amyloid

pathology. JAMA. 305:275-283.
Clark LJ, Gatz M, Zheng L, Chen YL, McCleary C, Mack WJ. 2009. Longitudinal verbal fluency in normal aging, preclinical, and prevalent Alzheimer's disease. Am J Alzheimers Dis Other Demen. 24:461-468.
Crystal H, Dickson D, Fuld P, Masur D, Scott R, Mehler M, Masdeu J, Kawas C, Aronson M, Wolfson L. 1988. Clinico-pathologic studies in dementia: nondemented subjects with pathologically confirmed Alzheimer's disease. Neurology. 38:1682-1687.
Davis DG, Schmitt FA, Wekstein DR, Markesbery WR. 1999. Alzheimer neuropathologic alterations in aged cognitively normal subjects. J Neuropathol Exp Neurol. 58:376-388.
Dickerson BC, Salat DH, Greve DN, Chua EF, Rand-Giovannetti E, Rentz DM, Bertram L, Mullin K, Tanzi RE, Blacker D, Albert MS, Sperling RA. 2005. Increased hippocampal activation in mild cognitive impairment compared to normal aging and AD. Neurology. 65:404-411.
Doraiswamy PM, Sperling RA, Coleman RE, Johnson KA, Reiman EM, Davis MD, Grundman M, Sabbagh MN, Sadowsky CH, Fleisher AS, Carpenter A, Clark CM, Joshi AD, Mintun MA, Skovronsky DM, Pontecorvo MJ. 2012. Amyloid-β assessed by florobetapir F 18 PET and 18-month cognitive decline: a multicenter study. Neurology. 79:1636-1644.
Driscoll I, Resnick SM, Troncoso JC, An Y, O'Brien R, Zonderman AB. 2006. Impact of Alzheimer's pathology on cognitive trajectories in nondemented elderly. Ann Neurol. 60:688-695.
Erickson KI, Voss MW, Prakash RS, Basak C, Szabo A, Chaddock L, Kim JS, Heo S, Alves H, White SM, Wojcicki TR, Mailey E, Vieira VJ, Martin SA, Pence BD, Woods JA, McAuley E, Kramer AF. 2011. Exercise training increases size of hippocampus and improves memory. Proc Natl Acad Sci U S A. 108:3017-3022.
Fleisher AS, Houston WS, Eyler LT, Frye S, Jenkins C, Thal LJ, Bondi MW. 2005. Identification of Alzheimer disease risk by functional magnetic resonance imaging. Arch Neurol. 62:1881-1888.
Freundlieb N, Philipp S, Schneider SA, Brüggemann N, Klein C, Gerloff C, Hummel FC. 2012. No association of the BDNF val66met polymorphism with implicit associative vocabulary and motor learning. PLoS One. 7:e48327.
Golby A, Silverberg G, Race E, Gabrieli S, O'Shea J, Knierim K, Stebbins G, Gabrieli J. 2005. Memory encoding in Alzheimer's disease: an fMRI study of explicit and implicit memory. Brain. 128:773-787.
Gorski JA, Zeiler SR, Tamowski S, Jones KR. 2003. Brain-derived neurotrophic factor is required for the maintenance of cortical dendrites. J Neurosci. 23:6856-6865.
Grady CL, Furey ML, Pietrini P, Horwitz B, Rapoport SI. 2001. Altered brain functional connectivity and impaired short-term memory in Alzheimer's disease. Brain. 124:739-756.
Grady CL, McIntosh AR, Beig S, Keightley ML, Burian H, Black SE. 2003. Evidence from functional neuroimaging of a compensatory prefrontal network in Alzheimer's disease. J Neurosci. 23:986-993.
Grossman M, Koenig P, Glosser G, DeVita C, Moore P, Rhee J, Detre J, Alsop D, Gee J. 2003a. Neural basis for semantic memory difficulty in Alzheimer's disease: an fMRI study. Brain. 126:292-311.
Grossman M, Koenig P, DeVita C, Glosser G, Moore P, Gee J, Detre J, Alsop D. 2003b. Neural basis for verb processing in Alzheimer's disease: an fMRI study. Neuropsychology. 17:658-674.
Hatashita S, Yamasaki H, Suzuki Y, Tanaka K, Wakebe D, Hayakawa H. 2014. [18F]Flutemetamol amyloid-beta PET imaging compared with [11C]PIB across the spectrum of Alzheimer's disease. Eur J Nucl Med Mol Imaging. 41:290-300.
Herholz K, Ebmeier K. 2011. Clinical amyloid imaging in Alzheimer's disease. Lancet Neurol. 10:667-670.
Howard D, Patterson KE. 1992. The Pyramids and Palm Trees Test: A test of semantic access from words and pictures. Bury St. Edmunds (UK): Thames Valley Test Company.
Huff FJ, Corkin S, Growdon JH. 1986. Semantic impairment and anomia in Alzheimer's disease. Brain Lang. 28:235-249.
Hyman BT, Kromer LJ, Van Hoesen GW. 1987. Reinnervation of the hippocampal perforant pathway zone in Alzheimer's disease. Ann Neurol. 21:259-267.
Johnson SC, Schmitz TW, Moritz CH, Meyerand ME, Rowley HA, Alexander AL, Hansen KW, Gleason CE, Carlsson CM, Ries ML, Asthana S, Chen K, Reiman EM, Alexander GE. 2006a. Activation of brain regions vulnerable to Alzheimer's disease: the effect of mild cognitive impairment. Neurobiol Aging. 27:1604-1612.
Johnson SC, Schmitz TW, Trivedi MA, Ries ML, Torgerson BM, Carlsson CM, Asthana S, Hermann BP, Sager MA. 2006b. The influence of Alzheimer disease family history and apolipoprotein E epsilon4 on mesial temporal lobe activation. J Neurosci. 26:6069-6076.
Katzman R, Terry R, DeTeresa R, Brown T, Davies P, Fuld P, Renbing X, Peck A. 1988. Clinical, pathological, and neurochemical changes in dementia: a subgroup with preserved mental status and numerous neocortical plaques. Ann Neurol. 23:138-144.
Kebir O, Mouaffak F, Chayet M, Leroy S, Tordjman S, Amado I, Krebs MO. 2009. Semantic but not phonological verbal fluency associated with BDNF Val66Met polymorphism in schizophrenia. Am J Med Genet B Neuropsychiatr Genet. 150B:441-442.
Koole M, Lewis DM, Buckley C, Nelissen N, Vandenbulcke M, Brooks DJ, Vandenberghe R, Van Laere K. 2009. Whole-body biodistribution and radiation dosimetry of 18F- GE067: a radioligand for in vivo brain amyloid imaging. J Nucl Med. 50:818-822.
Laiacona M, Capitani E. 2001. A case of prevailing deficit of nonliving categories or a case of prevailing sparing of living categories? Cogn Neuropsychol. 18:39-70.
Lehtovirta M, Soininen H, Helisalmi S, Mannermaa A, Helkala EL, Hartikainen P, Hänninen T, Ryynänen M, Riekkinen PJ. 1996. Clinical and neuropsychological characteristics in familial and sporadic Alzheimer's disease: relation to apolipoprotein E polymorphism. Neurology. 46:413-419.

Li N, Bartlett CW. 2012. Defining the genetic architecture of human developmental language impairment. Life Sci. 90:469-475.

Li Y, Luikart BW, Birnbaum S, Chen J, Kwon CH, Kernie SG, Bassel-Duby R, Parada LF. 2008. TrkB regulates hippocampal neurogenesis and governs sensitivity to antidepressive treatment. Neuron. 59:399-412.

Machulda MM, Ward HA, Borowski B, Gunter JL, Cha RH, O'Brien PC, Petersen RC, Boeve BF, Knopman D, Tang-Wai DF, Ivnik RJ, Smith GE, Tangalos EG, Jack JC. 2003. Comparison of memory fMRI response among normal, MCI, and Alzheimer's patients. Neurology. 61:500-506.

Mendez MF. 2012. Early-onset Alzheimer's disease: nonamnestic subtypes and type 2 AD. Arch Med Res. 43:677-685.

Mesulam MM. 1999. Neuroplasticity failure in Alzheimer's disease: bridging the gap between plaques and tangles. Neuron. 24:521-529.

Mez J, Cosentino S, Brickman AM, Huey ED, Mayeux R. 2013. Different demographic, genetic, and longitudinal traits in language versus memory Alzheimer's subgroups. J Alzheimers Dis. 37:137-146.

Mondadori CRA, Buchmann A, Mustovic H, Schmidt CF, Boesiger P, Nitsch RM, Hock C, Streff J, Henke K. 2006. Enhanced brain activity may precede the diagnosis of Alzheimer's disease by 30 years. Brain. 129:2908-2922.

Morris JC, Roe CM, Grant EA, Head D, Storandt M, Goate AM, Fagan AM, Holtz- man DM, Mintun MA. 2009. Pittsburgh compound B imaging and prediction of progression from cognitive normality to symptomatic Alzheimer disease. Arch Neurol. 66:1469-1475.

Müller-Gärtner HW, Links JM, Prince JL, Bryan RN, McVeigh E, Leal JP, Davatzikos C, Frost JJ. 1992. Measurement of radiotracer concentration in brain gray matter using positron emission tomography: MRI-based correction for partial volume effects. J Cereb Blood Flow Metab. 12:571-583.

Nathan BP, Bellosta S, Sanan DA, Weisgraber KH, Mahley RW, Pitas RE. 1994. Differential effects of apolipoproteins E3 and E4 on neuronal growth in vitro. Science. 264:850-852.

Nelissen N, Dupont P, Vandenbulcke M, Tousseyn T, Peeters R, Vandenberghe R. 2011. Right hemisphere recruitment during language processing in frontotemporal lobar degeneration and Alzheimer's disease. J Mol Neurosci. 45:637-647.

Nelissen N, Van Laere K, Thurfjell L, Owenius R, Vandenbulcke M, Koole M, Bormans G, Brooks DJ, Vandenberghe R. 2009. Phase 1 study of the Pittsburgh compound B derivative 18F-flutemetamol in healthy volunteers and patients with probable Alzheimer disease. J Nucl Med. 50:1251-1259.

Nelissen N, Vandenbulcke M, Fannes K, Verbruggen A, Peeters R, Dupont P, Van Laere K, Bormans G, Vandenberghe R. 2007. Abeta amyloid deposition in the language system and how the brain responds. Brain. 130:2055-2069.

Okuno H, Tokuyama W, Li YX, Hashimoto T, Miyashita Y. 1999. Quantitative evaluation of neurotrophin and trk mRNA expression in visual and limbic areas along the occipito-temporo-hippocampal pathway in adult macaque monkeys. J Comp Neurol. 408:378-398.

Osada T, Adachi Y, Kimura HM, Miyashita Y. 2008. Towards understanding of the cortical network underlying associative memory. Philos Trans R Soc Lond B Biol Sci. 363:2187-2199.

Pallier C. 2002. Computing discriminability and bias with the R software. URL http://www.pallier.org/ressources/aprime/aprime.pdf

Price CJ, Mechelli A. 2005. Reading and reading disturbance. Curr Opin Neurobiol. 15:231-238.

Price JL, Morris JC. 1999. Tangles and plaques in nondemented aging and "preclinical" Alzheimer's disease. Ann Neurol. 45:358-368.

Rasmusson DX, Dal Forno G, Brandt J, Warren AC, Troncoso J, Lyketsos C. 1996. Apo-E genotype and verbal deficits in Alzheimer's disease. J Neuropsychiatry Clin Neurosci. 8:335-337.

Reiman EM, Quiroz YT, Fleisher AS, Chen K, Velez-Pardo C, Jimenez-Del-Rio M, Fagan AM, Shah AR, Alvarez S, Arbelaez A, Giraldo M, Acosta-Baena N, Sperling RA, Dickerson B, Stern CE, Tirado V, Munoz C, Reiman RA, Huentelman MJ, Alexander GE, Langbaum JBS, Kosik KS, Tariot PN, Lopera F. 2012. Brain imaging and fluid biomarker analysis in young adults at genetic risk for autosomal dominant Alzheimer's disease in the presenilin 1 E280A kindred: a case-control study. Lancet Neurol. 11:1048-1056.

Resnick SM, Sojkova J, Zhou Y, An Y, Ye W, Holt DP, Dannals RF, Mathis CA, Klunk WE, Ferrucci L, Kraut MA, Wong DF. 2010. Longitudinal cognitive decline is associated with fibrillar amyloid-beta measured by [11C]PiB. Neurology. 74:807-815.

Ricci PT, Zelkowicz BJ, Nebes RD, Meltzer CC, Mintun MA, Becker JT. 1999. Functional neuroanatomy of semantic memory: recognition of semantic associations. Neuroimage. 9:88-96.

Saykin AJ, Flashman LA, Frutiger SA, Johnson SC, Mamourian AC, Moritz CH, O'Jile JR, Riordan HJ, Santulli RB, Smith CA, Weaver JB. 1999. Neuroanatomic substrates of semantic memory impairment in Alzheimer's disease: patterns of functional MRI activation. J Int Neuropsychol Soc. 5:377-392.

Seidenberg M, Guidotti L, Nielson KA, Woodard JL, Durgerian S, Antuono P, Zhang Q, Rao SM. 2009. Semantic memory activation in individuals at risk for developing Alzheimer disease. Neurology. 73:612-620.

Simmons TR, Flax JF, Azaro MA, Hayter JE, Justice LM, Petrill SA, Bassett AS, Tallal P, Brzustowicz LM, Bartlett CW. 2010. Increasing genotype-phenotype model determinism: application to bivariate reading/language traits and epistatic interactions in language-impaired families. Hum Hered. 70:232-244.

Small SA, Perera GM, DeLaPaz R, Mayeux R, Stern Y. 1999. Differential regional dysfunction of the hippocampal formation among elderly with memory decline and Alzheimer's disease. Ann Neurol. 45:466-472.

Snodgrass JG, Vanderwart M. 1980. A standardized set of 260 pictures: norms for name agreement, image agreement, familiarity, and visual complexity. J Exp Psychol Hum Learn. 6:174-215.

Sperling RA, Bates JF, Chua EF, Cocchiarella AJ, Rentz DM, Rosen BR, Schacter DL, Albert MS. 2003. fMRI studies of associative encoding in young and elderly controls and mild Alzheimer's disease. J Neurol Neurosurg Psychiatry.

74:44-50.
Sperling R. 2007. Functional MRI studies of associative encoding in normal aging, mild cognitive impairment, and Alzheimer's disease. Ann N Y Acad Sci. 1097:146-155.
Sperling RA, Aisen PS, Beckett LA, Bennett DA, Craft S, Fagan AM, Iwatsubo T, Jack J CR, Kaye J, Montine TJ, Park DC, Reiman EM, Rowe CC, Siemers E, Stern Y, Yaffe K, Carrillo MC, Thies B, Morrison-Bogorad M, Wagster MV, Phelps CH. 2011. Toward defining the preclinical stages of Alzheimer's disease: recommendations from the National Institute on Aging-Alzheimer's Association workgroups on diagnostic guidelines for Alzheimer's disease. Alzheimers Dement. 7:280-292.
Sugarman MA, Woodard JL, Nielson KA, Seidenberg M, Smith JC, Durgerian S, Rao SM. 2012. Functional magnetic resonance imaging of semantic memory as a presymptomatic biomarker of Alzheimer's disease risk. Biochim Biophys Acta. 1822:442-456.
Thurfjell L, Lilja J, Lundqvist R, Buckley C, Smith A, Vandenberghe R, Sherwin P. 2014. Automated Quantification of 18F-Flutemetamol PET Activity for Categorizing Scans as Negative or Positive for Brain Amyloid: Concordance with Visual Image Reads. J Nucl Med. 55:1623-8.
Troncoso JC, Martin LJ, Dal Forno G, Kawas CH. 1996. Neuropathology in controls and demented subjects from the Baltimore Longitudinal Study of Aging. Neurobiol Aging. 17:365-371.
Tzourio-Mazoyer N, Landeau B, Papathanassiou D, Crivello F, Etard O, Delcroix N, Mazoyer B, Joliot M. 2002. Automated anatomical labeling of activations in SPM using a macroscopic anatomical parcellation of the MNI MRI single-subject brain. Neuroimage. 15:273-289.
Vandenberghe R, Price C, Wise R, Josephs O, Frackowiak RS. 1996. Functional anatomy of a common semantic system for words and pictures. Nature. 383:254-256.
Vandenberghe R, Van Laere K, Ivanoiu A, Salmon E, Bastin C, Triau E, Hasselbalch S, Law I, Andersen A, Korner A, Minthon L, Garraux G, Nelissen N, Bormans G, Buckley C, Owenius R, Thurfjell L, Farrar G, Brooks DJ. 2010. 18F-flutemetamol amyloid imaging in Alzheimer disease and mild cognitive impairment: a phase 2 trial. Ann Neurol. 68:319-329.
Vandenberghe R, Wang Y, Nelissen N, Vandenbulcke M, Dhollander T, Sunaert S, Dupont P. 2013a. The associative-semantic network for words and pictures: effective connectivity and graph analysis. Brain Lang. 127:264-272.
Vandenberghe R, Nelissen N, Salmon E, Ivanoiu A, Hasselbalch S, Andersen A, Korner A, Minthon L, Brooks DJ, Van Laere K, Dupont P. 2013b. Binary classification of 18F-flutemetamol PET using machine learning: comparison with visual reads and structural MRI. Neuroimage. 64:517-525.
Vandenberghe R, Adamczuk K, Dupont P, Van Laere K, Chételat G. 2013c. Amyloid PET in clinical practice: Its place in the multidimensional space of Alzheimer's disease. Neuroimage Clin. 2:497-511.
Vandenberghe R, Adamczuk K, Van Laere K. 2013d. The interest of amyloid PET imaging in the diagnosis of Alzheimer's disease. Curr Opin Neurol. 26:646-655.
Vandenbulcke M, Peeters R, Dupont P, Van Hecke P, Vandenberghe R. 2007. Word reading and posterior temporal dysfunction in amnestic mild cognitive impairment. Cereb Cortex. 17:542-551.
Vandenbulcke M, Peeters R, Fannes K, Vandenberghe R. 2006. Knowledge of visual attributes in the right hemisphere. Nat Neurosci. 9:964-970.
Vandenbulcke M, Peeters R, Van Hecke P, Vandenberghe R. 2005. Anterior temporal laterality in primary progressive aphasia shifts to the right. Ann Neurol. 58:362-370.
Verhaeghen P, Vandenbroucke A, Dierckx V. 1998. Growing slower and less accurate: adult age differences in time-accuracy functions for recall and recognition from episodic memory. Exp Aging Res. 24:3-19.
Villemagne VL, Pike KE, Chételat G, Ellis KA, Mulligan RS, Bourgeat P, Ackermann U, Jones G, Szoeke C, Salvado O, Martins R, O'Keefe G, Mathis CA, Klunk WE, Ames D, Masters CL, Rowe CC. 2011. Longitudinal assessment of Aβ and cognition in aging and Alzheimer disease. Ann Neurol. 69:181-192.
Webster MJ, Herman MM, Kleinman JE, Shannon Weickert C. 2006. BDNF and trkB mRNA expression in the hippocampus and temporal cortex during the human lifespan. Gene Expr Patterns. 6:941-951.
Whitney C, Kirk M, O'Sullivan J, Lambon Ralph MA, Jefferies E. 2011. The neural organization of semantic control: TMS evidence for a distributed network in left inferior frontal and posterior middle temporal gyrus. Cereb Cortex. 21:1066-1075.
Whitney C, Kirk M, O'Sullivan J, Lambon Ralph MA, Jefferies E. 2012. Executive semantic processing is underpinned by a large-scale neural network: revealing the contribution of left prefrontal, posterior temporal, and parietal cortex to controlled retrieval and selection using TMS. J Cogn Neurosci. 24:133-147.
Woodard JL, Seidenberg M, Nielson KA, Antuono P, Guidotti L, Durgerian S, Zhang Q, Lancaster M, Hantke N, Butts A, Rao SM. 2009. Semantic memory activation in amnestic mild cognitive impairment. Brain. 132:2068-2078.